World Conference on Timber Engineering Oslo 2023

STUDY ON THE STRUCTURAL PERFORMANCE OF PLYWOOD BEARING WALL WITH THE RUSTED NAIL AND DECAYED WOOD

Yuki Ota[1], Hiroki Ishiyama[2], Shigefumi Okamoto[3]

ABSTRACT: In this study, based on the study of the past, deterioration degree of nail and wood is classified because there is a correlation between the maximum load and not only the deterioration degree of the nail by visual inspection but also the penetration depth by pilodyn measurement in the decayed part of wood[1)2)].
And the formula which predicts characteristic of a deformation-load relation when the nail rust and wood decay is developed. Also, using the result and analysing, the structural characteristic of the plywood bearing wall with the nails rusted wood decayed according to the degree of deterioration of the nail and wood can be predicted. As a result,

1. It is revealed that the maximum strength doesn't decrease remarkably when only the sill of plywood bearing wall deteriorates.
2. When the column deteriorates, the rigidity after yield is remarkably reduced.
3. even if the wood decay a little, the strength increases due to the influence of rusting of the nail, and it decreases when further deterioration progresses.

KEYWORDS: Wooden structure, Nail joint, Biological deterioration, Shear strength, Durability, Pull-out force

1 INTRODUCTION

Wooden houses may be required to ensure their safe and long-term use as living spaces. In the deterioration diagnosis currently used, bearing capacity of wall magnification is reduced based on the results of the determination of some deteriorated conditions, such as balconies. And wooden houses may not be adequately repaired according to the degree of deterioration.
So, the shear resistance of the nail joint with rusted nail and decayed wood is formulated based on the study of the past, and the structural characteristic of the plywood bearing wall according to the degree of deterioration of the nail and wood is estimated using the results.

2 ESTIMATION OF THE SHEAR CAPACITY OF JOINT

2.1 CLASSIFICATION OF DETERIORATION DEGREE

The deterioration degree is divided to concisely calculate the shear capacity of nail joint according to the deterioration degree. There is a correlation between the maximum load and the deterioration degree of the nail by visual inspection (Table 1[1)], Fig.1[2)]). And according to Fig.2, it is found that the same behaviour is shown in the case of the same deterioration degree of the nail. Also, there is a correlation between the maximum load and the penetration depth by pilodyn measurement in the decayed part of wood (Fig.3)[3)]. The degree of decay of wood is divided into four stages: pilodyn driving depth of less than 23.5 mm, 23.5 mm or more and less than 27.5 mm, 27.5 mm or more and less than 35 mm, and 35 mm or more. Separated in this way, from Fig.4, the test specimen at the same stage exhibits generally similar behavior. Therefore, the deterioration degree division is Table 2. However, in this study, it is dealt with the degree of deterioration shown in the shaded part of Table2, because moisture is the main cause of both rusting of nails and decay of wood and it is unlikely that only either of them is deteriorate significantly.

Table 1: *Standard of the deterioration grade*

Rating	Standard	Example
1	Scarcely rusted	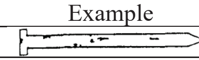
2	Partially rusted, no visible defect	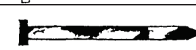
3	Totally rusted, no defect inside	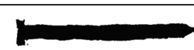
4	Partially defect, with original length	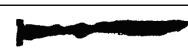
5	failure	

[1] Yuki Ota, Osaka Metropolitan University, Japan, uo49yfwhq9o75yuq98y@gmail.com
[2] Hiroki, Ishiyama, Osaka Metropolitan University, Japan, ishiyama@omu.ac.jp
[3] Shigefumi Okamoto, Osaka Metropolitan University, Japan, okmt@omu.ac.jp

https://doi.org/10.52202/069179-0344

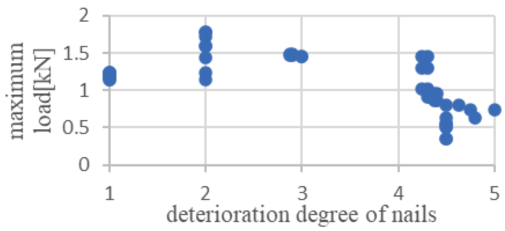

Figure 1: *A correlation between the maximum load and the deterioration degree of the nail*

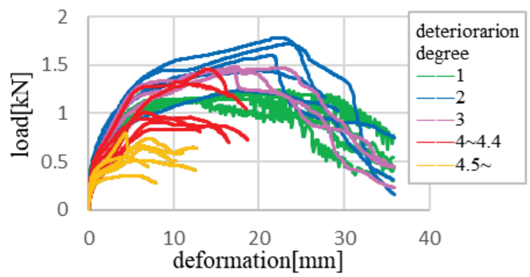

Figure 2: *Experimental results of unit joints with rusted nail*

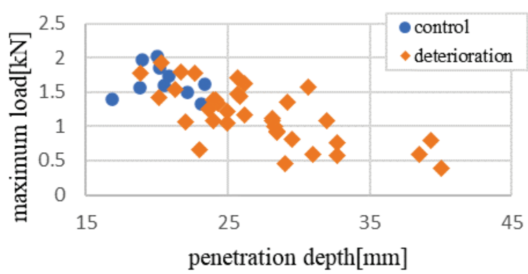

Figure 3: *A correlation between the maximum load and the penetration depth by pilodyn*

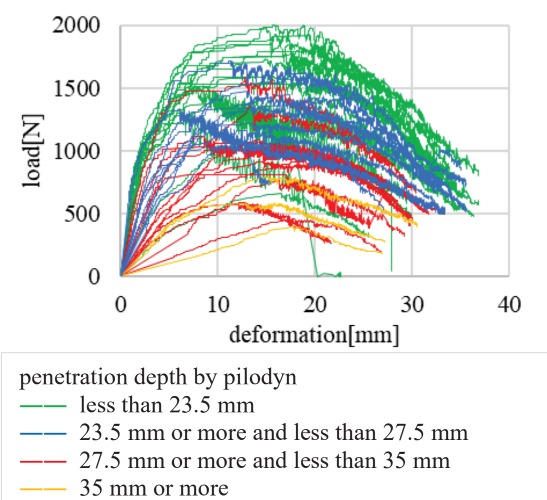

Figure 4: *Experimental results of unit joints with decayed wood*

Table 2: *Division of deterioration degree*

		Deterioration degree of nail					
		1	2	2.5 ~3.5	4 ~4.5		4.5~
Penetration depth[mm]	~23.5	Aa	Ba	Ca	Da	Ea	Fa
	23.5~27.5	Ab	Bb	Cb	Db	Eb	Fb
	27.5~35	Ac	Bc	Cc	Dc	Ec	Fc
	35~	Ad	Bd	Cd	Dd	Ed	Fd

2.2 ESTIMATION OF TENSILE STRENGTH WITH DETERIORATED NAIL AND WOOD

It is believed that when a shear load is added to the nail joint and the displacement increases, the deflection angle of the nail increases, and resulting in nail pull-out, punching out, or braking. Therefore, it is a breaking point where the axial force of the nail is reached either the pull-out stress intensity of the nail, the nail head penetration bearing capacity of plywood, or the tensile strength of the nail. And the nail head penetration strength of plywood and the tensile strength of nails are determined in the same manner as in previous studies [2)]. So, the penetration strength is determined as a stress intensity of 1404 N/mm^2 based on the experimental results of previous study[2)] and the tensile strength is calculated by multiplying the lower limit of the tensile strength ($690N/mm^2$) of the iron wire for nail (JISG3562 SWM-N) by the cross-sectional area of the nail body diameter. On the other hand, the pull-out stress intensity of the nail is determined by equation (1).

$$P_d = 4r\int_{\theta_1}^{\theta_2} F(\theta)\mu_{sta}(\theta)d\theta \qquad (1)$$

Where, $F(\theta)$ =uniaxial compressive strength of wood [kN], $\mu sta(\theta)$ = static friction coefficient, θ = angle [°] and r = nail radius [mm].

Therefore, the uniaxial compressive strength of wood, the coefficient of statin friction between the rusted nail and the wood, and the range which involved in pull-out resistance of nail (Fig.5) is determined from the study of the past[2)4)5)]. The method is shown below.

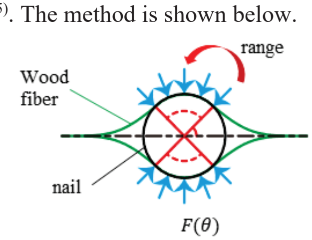

Figure 5: *Range which involved in pull-out resistance of nail*

2.2.1 Uniaxial compressive strength of wood

As for the uniaxial compressive strength, based on the research results[4)], the supporting strength of the wood in the parallel direction of the fiber and the direction in the direction of the fiber perpendicular is adopted. So, the uniaxial compressive strength of wood in fiber equilibrium direction and the fiber orthogonal direction is represented by the formula (2) and (3), respectively.

fiber equilibrium direction:

$$F_l = -0.7867(x - 20.5) + 35.655 \quad (2)$$

fiber orthogonal direction:

$$F_r = -1.0316(x - 20.5) + 41.271 \quad (3)$$

Where, x =penetration depth by pilodyn.

2.2.2 The coefficient of statin friction between no damage nail and wood

The coefficient of statin friction between no damage nail and wood is adopted by the study[5]. So, coefficient of statin friction between no damage nail and wood in fiber equilibrium direction and the fiber orthogonal direction is represented by the formula (4) and (5), respectively.

fiber equilibrium direction:

$$\mu_{sta_l} = -0.325r_u + 0.409 \quad (4)$$

fiber orthogonal direction:

$$\mu_{sta_r} = -0.386r_u + 0.318 \quad (5)$$

Where, r_u =specific gravity of wood.

2.2.3 The range which involved in pull-out resistance of nail

Using the Hankinson's equation, $F(\theta)$ and $\mu_{sta}(\theta)$ are presented by equation (6) and (7), respectively.

$$F(\theta) = \frac{F_l \times F_r}{F_l sin^2(\theta) + F_r cos^2(\theta)} \quad (6)$$

$$\mu_{sta}(\theta) = \frac{\mu_{sta_l} \times \mu_{sta_r}}{\mu_{sta_l} sin^2(\theta) + \mu_{sta_r} cos^2(\theta)} \quad (7)$$

Further, by substituting into equation (1), the following equation (8) is obtained.

$$P_d = 4r \int_{\theta_1}^{\theta_2} \frac{F_l \times F_r}{F_l sin^2(\theta) + F_r cos^2(\theta)} \times \frac{\mu_{sta_l} \times \mu_{sta_r}}{\mu_{sta_l} sin^2(\theta) + \mu_{sta_r} cos^2(\theta)} d\theta \quad (8)$$

From previous research[2], since the pull-out resistance of the CN65 nail (P_d) is 627.2[N], the required range is θ_{65}~90[°] satisfying equation (9).

$$627.2 = 4r_{65} \int_{\theta_{65}}^{90°} \frac{F_l \times F_r}{F_l sin^2(\theta) + F_r cos^2(\theta)} \times \frac{\mu_{sta_l} \times \mu_{sta_r}}{\mu_{sta_l} sin^2(\theta) + \mu_{sta_r} cos^2(\theta)} d\theta \quad (9)$$

Where, r_{65}=CN65 nail radius [mm]=1.665.
Here, when $\theta_{65} = 89.65°$ and when $\theta_{65} = 89.7°$, the value of equation (9) is 629.9 and 539.9, respectively. So, θ_{65} is found to be about 89.65°.

Then, a range of 89.95 ~ 90 [°] related to the extraction resistance in the case of CN65 nail is applied to the N50 nail. Assuming that the state of the wood when the wood fibers are pushed apart by driving a nail is the same as in the case of CN65 nail and N50 nail, the nail joint at that time is considered to be as shown in Fig.6.

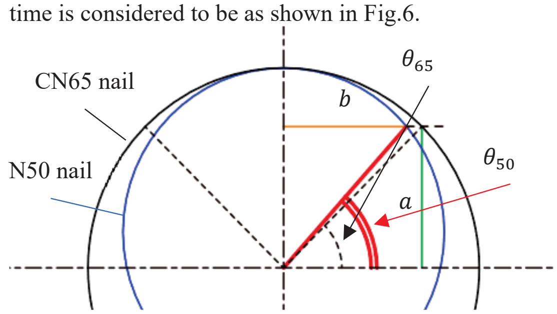

Figure 6: *Schematic of the nail joint when CN65 and N50 nails are driven into wood*

At the time, the range of θ_{50} ~90[°] that affects the extraction resistance in the case of the N 50 nail is represented by the formula (10).

$$\theta_{50} = \tan^{-1}\left(\frac{a}{b}\right) = \tan^{-1}\left(\frac{r_{65}\sin\theta_{65}}{\sqrt{{r_{50}}^2 - (r_{65}\sin\theta_{65} - r_{65} + r_{50})^2}}\right) \quad (10)$$

Where, r_{50}=N50 nail radius [mm]=1.375.
Therefore, when $\theta_{65} = 89.65°$ is substituted into equation (10), $\theta_{50} = 89.7°$, so the range which involved in pull-out resistance of N50 nail is revealed that 89.7~90[°].

2.2.4 The coefficient of statin friction between rusted nail and no damage wood

The coefficient of statin friction between rusted nail and no damage wood is determined based on the results of the pull-out experiment about CN65 nail in previous study[2]. The method is shown below. First, it is calculated how many times the static friction coefficient between rusted nail and no damage wood is that between no damage nail and wood in the case of CN65 nail. Assuming that the rate of increasing static friction is expressed by equation (11), the weight remaining rate of the nail and the rate are shown in Table 3 from the experimental study[2].

$$R = M_R / M_N \quad (11)$$

Where, R =rate of increasing static friction, M_R = maximum pull-out strength with rusted nail and M_N = maximum pull-out strength with no damage nail.
And, assuming that the corrosion depth of the nails when the degree of deterioration of the nails is the same, the weight residual rate of N50 nails having a corrosion depth equivalent to that of CN65 nails with a certain weight residual rate is calculated. The schematic diagram of the rusted nail looks like Fig. 7, so if the nail rust occurs uniformly throughout the nail, the corrosion depth is expressed by formula (12).

https://doi.org/10.52202/069179-0344

***Table 3:** static friction (CN65 nail)*

Weight Residual rate	Maximum pull-out strength	Rate of Increasing static friction
100.00[%]	627.2[N]	1.00
97.3[%]	1821.8[N]	2.90
93.4[%]	3011.5[N]	4.80
83.5[%]	3405.1[N]	5.43

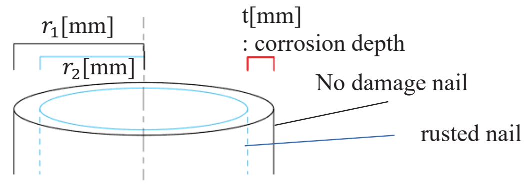

***Figure 7:** Schematic of rusted nails*

$$t = r_1(1 - \sqrt{q}) \tag{12}$$

Where, r_1=body diameter of no damage nail, r_2=body diameter of rusted nail and q=weight residual ratio $= \frac{{r_2}^2}{{r_1}^2}$. Therefore, when the corrosion depths of the CN65 nail and the N50 nail are equal, the weight residual ratio of the N50 nail is expressed by Equation (13).

$$q_{50} = \left\{1 + \frac{r_{65}}{r_{50}}\left(\sqrt{q_{65}} - 1\right)\right\}^2 \tag{13}$$

Where, q_{65} =weight residual ratio of CN65 nail, q_{50}=weight residual ratio of N50 nail, r_{65}= body diameter of CN65 nail and r_{50}= body diameter of N50 nail.
And the rate of increasing static friction of N50 nail at the time of nail rusting is shown in Table 4.

***Table 4:** static friction (N50 nail)*

Weight Residual rate	Rate of Increasing static friction
100.00[%]	1.00
96.74[%]	2.90
92.03[%]	4.80
80.21[%]	5.43

2.3 THE FORMULA OF DEFORMATION-LOAD RELATION

2.3.1 Creating formula on two-later ground

The formula which predicts change of a deformation-load relation when the nail rust and wood decay is developed by expanding the study of the past[2]. In other words, assuming that wood is a two-layer configuration of the decay part and the no damage part, using the horizontal resistance calculation formula of piles[6], the wood is regarded as the ground and the nail is regarded as the piles, and formulas are created for each protruding and fixing conditions of the nail head on two-layer ground. Therefore, equations (14), (15) and (16) are solved for the boundary conditions in the assumed nail head state, and constants A_n, B_n, C_n, and D_n satisfying these conditions are calculated.

$$\begin{aligned} y_1(x) = A_n e^{\beta_1 x}\cos(\beta_1 x) + B_n e^{\beta_1 x}\sin(\beta_1 x) \\ + C_n e^{-\beta_1 x}\cos(\beta_1 x) \\ + D_n e^{-\beta_1 x}\sin(\beta_1 x) \end{aligned} \tag{14}$$

$$\begin{aligned} y_2(x) = A_{n+1} e^{\beta_2 x} cos(\beta_2 x) + B_{n+1} e^{\beta_2 x} sin(\beta_2 x) \\ + C_{n+1} e^{-\beta_2 x} cos(\beta_2 x) \\ + D_{n*1} e^{-\beta_2 x} sin(\beta_2 x) \end{aligned} \tag{15}$$

$$y_3(x) = A_{n+2} + B_{n+2}x + C_{n+2}x^2 + D_{n+2}x^3 \tag{16}$$

Where, fixed numbers are shown in Table 5~8.

***Table 5:** Fixed number (1)*

H	N	Load
H_0	N	Load at the nail head
y_n	mm	Horizontal displacement of the nail in nth layer
x	mm	Depth
θ	rad	Nail angle
θ_0	rad	Nail head angle
M	$N \cdot mm$	Moment
M_0	$N \cdot mm$	Moment at the nail head
Kh_1	N/mm^2	Horizontal ground reaction coefficient of no damage wood at depth of $x[mm]$
Kh_2	N/mm^2	Horizontal ground reaction coefficient of decayed wood at depth of $x[mm]$
B	mm	Body diameter of nail
E	N/mm^2	Young's modulus of nail = 160000
I	mm^4	Moment of inertia of area of nail
ℓ	mm	Depth to boundary between no damage part and decayed part of wood
ℓ_m	mm	Depth of maximum moment occurrence
h	mm	Nail protrusion depth
$\beta_1 = \sqrt[4]{\frac{Kh_1}{EI}}$, $\beta_2 = \sqrt[4]{\frac{Kh_2}{EI}}$		
$\mathrm{F} = \frac{H}{4EI{\beta_1}^3}$, $\mathrm{F}' = \frac{H}{4EI{\beta_2}^3}$		
$a_1 = e^{\beta_1 \ell}$, $a_2 = e^{\beta_1 \ell}$		
$b_1 = a_1 a_2 + 4sin(\beta_1 \ell)cos(\beta_1 \ell)$ $b_2 = a_1 a_2 - 4sin(\beta_1 \ell)cos(\beta_1 \ell)$ $b_3 = {a_1}^2 - 4sin^2(\beta_1 \ell)$, $b_4 = {a_2}^2 + 4sin^2(\beta_1 \ell)$ $b_5 = {a_1}^2 + 4cos^2(\beta_1 \ell)$, $b_6 = {a_2}^2 - 4sin^2(\beta_1 \ell)$		
$c_1 = \beta_1\beta_2 b_3 + {\beta_2}^2 b_1$, $c_2 = {\beta_1}^2 b_2 + \beta_1\beta_2 b_3$ $c_3 = \beta_1\beta_2 b_2 + {\beta_2}^2 b_6$, $c_4 = {\beta_1}^2 b_4 + \beta_1\beta_2 b_2$ $c_5 = \beta_1\beta_2 b_1 + {\beta_2}^2 b_4$, $c_6 = {\beta_1}^2 b_6 + \beta_1\beta_2 b_1$ $c_7 = \beta_1\beta_2 b_2 + {\beta_2}^2 b_5$, $c_8 = \beta_1\beta_2 b_2 - {\beta_2}^2 b_5$ $c_9 = {\beta_1}^2 b_4 - \beta_1\beta_2 b_2$, $c_{10} = {\beta_1}^2 b_2 + \beta_1\beta_2 b_5$ $c_{11} = \beta_1\beta_2 b_4 + {\beta_2}^2 b_2$, $c_{12} = {\beta_1}^2 b_3 + \beta_1\beta_2 b_1$ $c_{13} = \beta_1\beta_2 b_2 + {\beta_2}^2 b_3$, $c_{14} = {\beta_1}^2 b_1 + \beta_1\beta_2 b_4$ $c_{15} = \beta_1\beta_2 b_6 + {\beta_2}^2 b_1$		

Table 6: *Fixed number (2)*

$d_1 = \beta_1\beta_2{}^2 b_2 + \beta_2{}^3 b_3,\ d_2 = \beta_1{}^3 b_1 + \beta_2{}^3 b_3$
$d_3 = \beta_1\beta_2{}^2 b_4 + \beta_2{}^3 b_2,\ d_4 = \beta_1{}^3 b_6 + \beta_2{}^3 b_2$
$d_5 = \beta_1\beta_2{}^2 b_4 - \beta_2{}^3 b_2,\ d_6 = \beta_1{}^3 b_6 - \beta_2{}^3 b_2$
$f_1 = a_2 d_1 sin(\beta_1\ell) + \beta_1 a_1 c_1 cos(\beta_1\ell)$
$f_2 = a_2 d_2 sin(\beta_1\ell) - \beta_1 a_1 c_2 cos(\beta_1\ell)$
$f_3 = d_3 i_1 - \beta_1 c_7 i_2,\ f_4 = d_4 i_1 + \beta_1 c_4 i_2$
$f_5 = f_3 + f_4,\ f_6 = f_3 - f_4$
$f_7 = d_5 i_1 + \beta_1 c_8 i_2,\ f_8 = d_6 i_1 + \beta_1 c_9 i_2$
$g_1 = \beta_2{}^2 a_2 c_2 sin(\beta_1\ell) + \beta_1{}^2 a_1 c_1 cos(\beta_1\ell)$
$g_2 = \beta_1{}^2 a_2 c_1 sin(\beta_1\ell) + \beta_2{}^2 a_1 c_2 cos(\beta_1\ell)$
$h_1 = c_1 d_2 + c_2 d_1$
$h_2 = \beta_1{}^2 a_2 f_1 sin(\beta_1\ell) + \beta_2{}^2 a_1 f_2 cos(\beta_1\ell)$
$h_3 = -\beta_2{}^2 a_2 f_3 sin(\beta_1\ell) + \beta_1{}^2 a_1 f_1 cos(\beta_1\ell)$
$h_4 = c_4 d_3 + c_7 d_4$
$h_5 = \beta_1{}^2 a_2 f_3 sin(\beta_1\ell) + \beta_2{}^2 a_1 f_4 cos(\beta_1\ell)$
$h_6 = \beta_1{}^2\{(a_1 + a_2) sin(\beta_1\ell) - a_2 cos(\beta_1\ell)\} f_3 + \beta_2{}^2\{a_1 sin(\beta_1\ell) + (a_1 + a_2) cos(\beta_1\ell)\} f_4$
$h_7 = c_7 d_5 + c_8 d_3,\ h_8 = c_4 d_6 - c_9 d_4$
$h_9 = c_7 d_6 + c_9 d_3,\ h_{10} = c_4 d_5 - c_8 d_4$
$h_{11} = c_8 d_6 - c_9 d_5$
$i_1 = a_1 sin(\beta_1\ell) + a_2 cos(\beta_1\ell)$
$i_2 = a_1 sin(\beta_1\ell) - a_2 cos(\beta_1\ell)$
$j_1 = f_5 h_{10} - f_6 h_7,\ j_2 = f_5 h_8 - f_6 h_9$
$j_3 = f_3 h_{10} + f_4 h_7,\ j_4 = f_3 h_8 + f_4 h_9$
$j_5 = f_5 h_9 - f_6 h_7,\ j_6 = f_5 h_8 - f_6 h_{10}$
$j_7 = f_3 h_7 - f_4 h_9,\ j_8 = f_3 h_{10} - f_4 h_8$
$G_1 = j_1 sin(\beta_2\ell) + j_2 cos(\beta_2\ell)$
$G_2 = j_2 sin(\beta_2\ell) - j_1 cos(\beta_2\ell)$
$G_3 = \{f_5 sin(\beta_2\ell) + f_6 cos(\beta_2\ell)\} h_4$
$G_4 = \{f_6 sin(\beta_2\ell) - f_5 cos(\beta_2\ell)\} h_4$
$G_5 = j_3 sin(\beta_2\ell) + j_4 cos(\beta_2\ell)$
$G_6 = j_4 sin(\beta_2\ell) - j_3 cos(\beta_2\ell)$
$G_7 = \{f_4 sin(\beta_2\ell) + f_3 cos(\beta_2\ell)\} h_4$
$G_8 = \{f_3 sin(\beta_2\ell) - f_4 cos(\beta_2\ell)\} h_4$
$G_9 = j_5 sin(\beta_2\ell) + j_6 cos(\beta_2\ell)$
$G_{10} = j_6 sin(\beta_2\ell) - j_5 cos(\beta_2\ell)$
$G_{11} = \{f_5 sin(\beta_2\ell) + f_6 cos(\beta_2\ell)\} h_{11}$
$G_{12} = \{f_6 sin(\beta_2\ell) - f_5 cos(\beta_2\ell)\} h_{11}$
$G_{13} = j_7 sin(\beta_2\ell) + j_8 cos(\beta_2\ell)$
$G_{14} = j_8 sin(\beta_2\ell) - j_7 cos(\beta_2\ell)$
$G_{15} = \{f_3 sin(\beta_2\ell) - f_4 cos(\beta_2\ell)\} h_{11}$
$G_{16} = \{f_4 sin(\beta_2\ell) + f_3 cos(\beta_2\ell)\} h_{11}$
$J_1 = G_5 e^{\beta_2(2\ell-\ell_m)} + G_7 e^{\beta_2\ell_m}$
$J_2 = G_1 e^{\beta_2(2\ell-\ell_m)} - G_3 e^{\beta_2\ell_m}$
$J_3 = G_6 e^{\beta_2(2\ell-\ell_m)} + G_8 e^{\beta_2\ell_m}$
$J_4 = G_2 e^{\beta_2(2\ell-\ell_m)} - G_4 e^{\beta_2\ell_m}$
$J_5 = G_{13} e^{\beta_2(\ell_m-2\ell)} + G_{15} e^{-\beta_2\ell_m}$
$J_6 = G_9 e^{\beta_2(\ell_m-2\ell)} + G_{11} e^{-\beta_2\ell_m}$
$J_7 = G_{14} e^{\beta_2(\ell_m-2\ell)} - G_{16} e^{-\beta_2\ell_m}$
$J_8 = G_{10} e^{\beta_2(\ell_m-2\ell)} + G_{12} e^{-\beta_2\ell_m}$
$p_1 = f_5 f_8 - f_6 f_7,\ p_2 = f_3 f_7 - f_4 f_8$

Table 7: *Fixed number (3)*

$q_1 = \beta_1{}^2 i_2 j_3 + \beta_2{}^2 i_1 j_4$
$q_2 = (\beta_1{}^2 f_4 i_2 + \beta_2{}^2 f_3 i_1) h_4$
$q_3 = \beta_1{}^2 i_2 j_1 + \beta_2{}^2 i_1 j_2$
$q_4 = (\beta_1{}^2 f_5 i_2 + \beta_2{}^2 f_6 i_1) h_4$
$q_5{}' = p_1(-\beta_1{}^2 i_2 j_7 + \beta_2{}^2 i_1 j_8) + p_2(\beta_1{}^2 i_2 j_5 - \beta_2{}^2 i_1 j_6)$
$q_6{}' = p_1(\beta_1{}^2 f_3 i_2 + \beta_2{}^2 f_4 i_1) h_{11} - p_2(\beta_1{}^2 f_5 i_2 - \beta_2{}^2 f_6 i_1) h_{11}$
$q_7 = \beta_1{}^2 i_2 j_5 - \beta_2{}^2 i_1 j_6$
$q_8 = (\beta_1{}^2 f_5 i_2 - \beta_2{}^2 f_6 i_1) h_{11}$
$q_9 = \beta_1{}^2 a_2 j_3 sin(\beta_1\ell) + \beta_2{}^2 a_1 j_4 cos(\beta_1\ell)$
$q_{10} = \{\beta_1{}^2 a_2 f_4 sin(\beta_1\ell) + \beta_2{}^2 a_1 f_3 cos(\beta_1\ell)\} h_4$
$q_{11} = \beta_1{}^2 a_2 j_1 sin(\beta_1\ell) + \beta_2{}^2 a_1 j_2 cos(\beta_1\ell)$
$q_{12} = \{\beta_1{}^2 a_2 f_5 sin(\beta_1\ell) + \beta_2{}^2 a_1 f_6 cos(\beta_1\ell)\} h_4$
$q_{13}{}' = p_1\{\beta_1{}^2 a_2 j_7 sin(\beta_1\ell) - \beta_2{}^2 a_1 j_8 cos(\beta_1\ell)\} - p_2\{\beta_1{}^2 a_2 j_5 sin(\beta_1\ell) - \beta_2{}^2 a_1 j_6 cos(\beta_1\ell)\}$
$q_{14}{}' = p_1\{\beta_1{}^2 a_2 f_3 sin(\beta_1\ell) + \beta_2{}^2 a_1 f_4 cos(\beta_1\ell)\} h_{11} - p_2\{\beta_1{}^2 a_2 f_5 sin(\beta_1\ell) - \beta_2{}^2 a_1 f_6 cos(\beta_1\ell)\} h_{11}$
$q_{15} = \beta_1{}^2 a_2 j_5 sin(\beta_1\ell) - \beta_2{}^2 a_1 j_6 cos(\beta_1\ell)$
$q_{16} = \{\beta_1{}^2 a_2 f_5 sin(\beta_1\ell) - \beta_2{}^2 a_1 f_6 cos(\beta_1\ell)\} h_{11}$
$Q_1 = 4\beta_1{}^2 e^{\beta_2(\ell-\ell_m)} \times \frac{(f_3{}^2 + f_4{}^2)}{J_1 J_4 - J_2 J_3}$
$Q_2 = \frac{1}{sin(\beta_2\ell_m)} \times \frac{G_3}{J_1 J_4 - J_2 J_3}$
$Q_3{}' = 4\beta_1{}^2 e^{\beta_2(\ell_m-\ell)} \times \frac{1}{J_5 J_8 - J_6 J_7}$
$Q_4 = \frac{1}{sin(\beta_2\ell_m)} \times \frac{G_{11}}{J_5 J_8 - J_6 J_7}$
$\mathcal{R}_1 = Q_1 e^{\beta_2\ell}\{q_1 e^{\beta_2(2\ell-\ell_m)} + q_2 e^{\beta_2\ell_m}\}$
$\mathcal{R}_2 = Q_2 e^{\beta_2\ell}\{q_3 e^{\beta_2(2\ell-\ell_m)} - q_4 e^{\beta_2\ell_m}\}$
$\mathcal{R}_3 = Q_3{}' e^{-\beta_2\ell}\{q_5{}' e^{\beta_2(\ell_m-2\ell)} - q_6{}' e^{-\beta_2\ell_m}\}$
$\mathcal{R}_4 = Q_4 e^{-\beta_2\ell}\{q_7 e^{\beta_2(\ell_m-2\ell)} + q_8 e^{-\beta_2\ell_m}\}$
$\mathcal{R}_5 = Q_1 e^{\beta_2\ell}\{q_9 e^{\beta_2(2\ell-\ell_m)} + q_{10} e^{\beta_2\ell_m}\}$
$\mathcal{R}_6 = Q_2 e^{\beta_2\ell}\{q_{11} e^{\beta_2(2\ell-\ell_m)} - q_{12} e^{\beta_2\ell_m}\}$
$\mathcal{R}_7 = Q_3{}' e^{-\beta_2\ell}\{q_{13}{}' e^{\beta_2(\ell_m-2\ell)} + q_{14}{}' e^{-\beta_2\ell_m}\}$
$\mathcal{R}_8 = Q_4 e^{-\beta_2\ell}\{q_{15} e^{\beta_2(\ell_m-2\ell)} + q_{16} e^{-\beta_2\ell_m}\}$
$S_1 = f_5 sin(\beta_2\ell) + f_6 cos(\beta_1\ell)$
$S_2 = f_6 sin(\beta_2\ell) - f_5 cos(\beta_1\ell)$
$S_3 = (-f_3 + 3f_4) sin(\beta_2\ell) + f_6 cos(\beta_1\ell)$
$S_4 = f_6 sin(\beta_2\ell) + (f_3 - 3f_4) cos(\beta_1\ell)$
$t_1 = \beta_1{}^2 a_2 sin(\beta_1\ell) + \beta_1\beta_2 i_2 - \beta_2{}^2 a_1 cos(\beta_1\ell)$
$t_2 = \beta_1{}^2 i_2 - 2\beta_1\beta_2 a_1 cos(\beta_1\ell) - \beta_2{}^2 i_1$
$t_3 = \beta_1{}^2 a_1 cos(\beta_1\ell) + \beta_1\beta_2 i_1 + \beta_2{}^2 a_2 sin(\beta_1\ell)$
$t_4 = \beta_1{}^2 i_1 + 2\beta_1\beta_2 a_2 sin(\beta_1\ell) + \beta_2{}^2 i_2$
$u_1 = \beta_1{}^3 i_1 + \beta_1{}^2\beta_2 a_2 sin(\beta_1\ell) + \beta_2{}^3 a_1 cos(\beta_1\ell)$
$u_2 = 2\beta_1{}^3 a_2 sin(\beta_1\ell) + \beta_1{}^2\beta_2 i_2 + \beta_2{}^3 i_1$
$u_3 = \beta_1{}^3 i_2 - \beta_1{}^2\beta_2 a_1 cos(\beta_1\ell) + \beta_2{}^3 a_2 sin(\beta_1\ell)$
$u_4 = 2\beta_1{}^3 a_1 cos(\beta_1\ell) + \beta_1{}^2\beta_2 i_1 - \beta_2{}^3 i_2$

https://doi.org/10.52202/069179-0344

Table 8: Fixed number (4)

$v_1 = {\beta_1}^3\beta_2 b_4 + 2{\beta_1}^2{\beta_2}^2 b_2 + \beta_1{\beta_2}^3 b_5$ $v_2 = {\beta_1}^3\beta_2 b_4 - \beta_1{\beta_2}^3 b_5$ $v_3 = {\beta_1}^3\beta_2 b_2 + 2{\beta_1}^2{\beta_2}^2 b_3 + \beta_1{\beta_2}^3 b_1$ $v_4 = {\beta_1}^3\beta_2 b_2 - \beta_1{\beta_2}^3 b_1$ $v_5 = {\beta_1}^3\beta_2 b_6 + 2{\beta_1}^2{\beta_2}^2 b_1 + \beta_1{\beta_2}^3 b_4$ $v_6 = {\beta_1}^3\beta_2 b_6 - \beta_1{\beta_2}^3 b_4$
$T_1 = t_1u_2 - t_2u_1,\ T_2 = t_1u_3 + t_3u_1$ $T_3 = -t_1u_4 + t_4u_1$
$U_1 = c_{12}T_1 - c_{10}T_2,\ U_2 = c_{13}T_1 - c_{11}T_2$ $U_3 = c_{14}T_1 - c_{10}T_3,\ U_4 = c_{15}T_1 - c_{11}T_3$ $U_5 = c_{14}T_2 - c_{12}T_3,\ U_6 = c_{15}T_2 - c_{13}T_3$
$V_1 = sin(\beta_2\ell) + cos(\beta_2\ell)$ $V_2 = sin(\beta_2\ell) - cos(\beta_2\ell)$
$W_1 = {\beta_1}^2\hbar^2(-{\beta_1}^2U_2V_2 + {\beta_2}^2U_1V_1) + \beta_1\hbar(-{\beta_1}^2U_4V_2 + {\beta_2}^2U_3V_1) + (-{\beta_1}^2U_6V_2 + {\beta_2}^2U_5V_1)$ $W_2 = {\beta_1}^2\hbar^2(-{\beta_1}^2U_2V_1 + {\beta_2}^2U_1V_2) + \beta_1\hbar(-{\beta_1}^2U_4V_1 + {\beta_2}^2U_3V_2) + (-{\beta_1}^2U_6V_1 + {\beta_2}^2U_5V_2)$
$X_1 = W_1 sin(\beta_2\ell) + W_2\,cos(\beta_2\ell)$ $X_2 = W_2 sin(\beta_2\ell) - W_1\,cos(\beta_2\ell)$
$Y_1 = {\beta_1}^2\hbar^2(-{\beta_1}^2U_2X_1 - {\beta_2}^2U_1X_2) + \beta_1\hbar(-{\beta_1}^2U_4X_1 - {\beta_2}^2U_3X_2) + (-{\beta_1}^2U_6X_1 - {\beta_2}^2U_5X_2)$

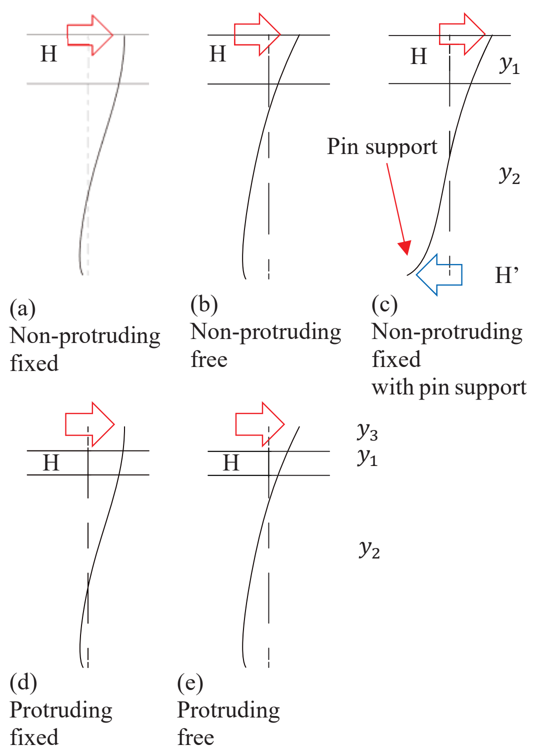

***Figure 8:** Schematic diagram of the nail joint under all nail head conditions*

2.3.1.1. Non-protruding and fixed

Fig. 8 (a) shows a nail joint when the nail head condition is non-protruding and fixed. The boundary conditions at this time are that θ_0=0 $[rad]$ and the horizontal load at the nail head is $H[N]$. And the calculations are equation (17) and (18).

$$y_1(0) = \frac{b_2h_1 + 8h_3}{4EI{\beta_1}^3 b_3h_1}H \tag{17}$$

$$H_0 = -\frac{2\beta_1 b_3 h_1}{b_1h_1 - 8h_2}M_0 \tag{18}$$

2.3.1.2. Non-protruding and free

Fig. 8 (b) shows a nail joint when the nail head condition is non-protruding and free. The boundary conditions at this time are that M_0=0 $[N \cdot mm]$ and the horizontal load at the nail head is $H[N]$. And the calculations are equation (19) ~ (22).

$$y_1(0) = \frac{b_4h_4 + 4h_5 - 4h_6}{2EI{\beta_1}^3 b_2h_4}H \tag{19}$$

$$\ell_m = \frac{1}{\beta_2}tan^{-1}\left(-\frac{f_5 sin(\beta_2\ell) + f_6 cos(\beta_2\ell)}{f_6 sin(\beta_2\ell) - f_5 cos(\beta_2\ell)}\right) \tag{20}$$

$$H(\ell_m) = \frac{\beta_1 M(\ell_m)(f_5 sin(\beta_2\ell) + f_6 cos(\beta_2\ell))h_4}{2{\beta_2}^2({f_3}^2 + {f_4}^2)sin(\beta_2\ell_m)}e^{\beta_2\ell_m - \beta_2\ell} \tag{21}$$

$$H(0) = \frac{\beta_1 M(0)h_4}{2{\beta_2}^2 f_4} \tag{22}$$

2.3.1.3. Non-protruding and free with pin support

Fig. 8 (c) shows a nail joint when the nail head condition is non-protruding and free with pin support in no damage part of wood. The boundary conditions at this time are that M_0=0 $[N \cdot mm]$, $M(\ell_m) = 0$, the horizontal load at the nail head is $H[N]$ and the horizontal load at ℓ_m is $H'[N]$. And the calculations are equation (23) ~ (25).

$$y_1(0) = \frac{{\beta_1}^2 b_4 + R_1 + R_3}{2EI{\beta_1}^5 b_2}H + \frac{R_2 + R_4}{2EI{\beta_1}^2{\beta_2}^3 b_2}H' \tag{23}$$

$$\theta(0) = \frac{{\beta_1}^2 b_1 + 2R_5 - 2R_7}{2EI{\beta_1}^4 b_2}H + \frac{R_6 + R_8}{2EI\beta_1{\beta_2}^3 b_2}H' \tag{24}$$

$$\theta(\ell_m) = \frac{S_1 - S_3}{2EI{\beta_1}^3} \times \frac{\beta_2 \sin(\beta_2\ell_m)}{f_5 \sin(\beta_2\ell) + f_6 \cos(\beta_2\ell)}H + \frac{S_2 + S_4}{2EI{\beta_2}^2} \times \frac{sin(\beta_2\ell_m)}{f_5 sin(\beta_2\ell) + f_6 cos(\beta_2\ell)}H' \tag{25}$$

2.3.1.4. Protruding and fixed

Fig. 8 (d) shows a nail joint when the nail head condition is protruding and fixed. The boundary conditions at this time are that $M(-h)$=0 $[rad]$ and the horizontal load at the nail head is $H[N]$. And the calculations are equation (26) ~ (29).

$$\ell_m = \frac{1}{\beta_2} tan^{-1}\left(\frac{W_1}{W_2}\right) \tag{26}$$

$$H_{\ell_m} = \frac{4{\beta_1}^3 M(\ell_m) t_1(\beta_1 \hbar T_1 + T_2) W_1 e^{\beta_2(\ell_m - \ell)}}{Y_1 sin(\beta_2 \ell_m)} \tag{27}$$

$$y_3(-h) = \frac{H}{12EI{\beta_1}^3 t_1(\beta_1 h T_1 + T_2)} \times \left\{ \begin{array}{c} {\beta_1}^4 h^4 t_1 T_1 + 4{\beta_1}^3 h^3 t_1 T_2 \\ +3{\beta_1}^2 h^2 (t_1 T_3 + t_2 T_2 + t_3 T_1) \\ +3\beta_1 h(t_2 T_3 + t_4 T_1) + 3(-t_3 T_3 + t_4 T_2) \end{array} \right\} \tag{28}$$

$$H_\ell = -\frac{4\beta_1 M(\ell) t_1(\beta_1 h T_1 + T_2)}{{\beta_1}^2 h^2 U_2 + \beta_1 h U_4 + U_6} \tag{29}$$

2.3.1.5. Protruding and free

Fig. 8 (e) shows a nail joint when the nail head condition is protruding and free. The boundary conditions at this time are that $\theta(-h)$=0 $[rad]$ and the horizontal load at the nail head is $H[N]$. And the calculations are equation (30) and (31).

$$y_3(-h) = \frac{1}{12EI{\beta_1}^3 t_1 T_1}\{4{\beta_1}^3 h^3 t_1 T_1 + 12{\beta_1}^2 h^2 t_1 T_2 + 6\beta_1 h(t_1 T_3 + t_2 T_2 + t_3 T_1) + 3(t_2 T_3 + t_4 T_1)\}H \tag{30}$$

$$y_3{}'(-h) = -\frac{{\beta_1}^2 h^2 T_1 + 2\beta_1 h T_2 + T_3}{2EI{\beta_1}^2 T_1} H \tag{31}$$

2.3.2 The formula deformation-load relation

Fixed numbers are shown in Table 9.

Table 9: *Fixed number (5)*

H_n	Horizontal load of the nail head at the nth change point of the load-deformation relationship
y_n	Horizontal displacement of the nail head at the nth change point of the load-deformation relationship
σ_{yp}	Yield stress of plywood to the nail side =4105
A_p	Cross-sectional area of plywood to the nail side
Z_n	Section modulus of nail
σ_n	Yield stress of nail =734.6
P_d	Pull-out stress intensity of the nail
P_h	The nail head penetration bearing capacity of plywood
P_n	The tensile strength of the nail

2.3.2.1. No damage wood and rusted nail

Fig.9 is a schematic of no damage wood and rusted nail using plywood as the side material. In this case, first, the wood yield in the state where the nail head is non-protruding and fixed, then the nail yield in the state of nail head protruding and fixed. And the finally, the nail is pulled out, the nail is broken, or the nail head is punching out in the state of nail head protruding and free. The horizontal load and horizontal displacement of the nail head at these times are expressed by equation (32) ~ (37), respectively.

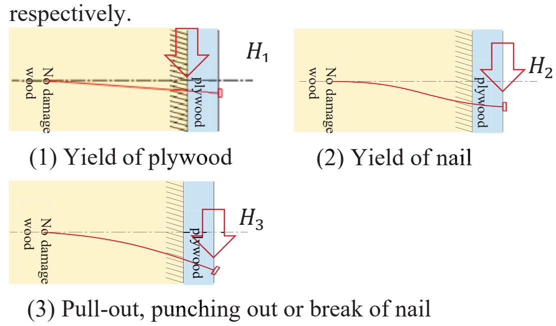

Figure 9: *No damage wood and rusted nail*

$$H_1 = \frac{\sigma_{yp} \times A_p}{2} \tag{32}$$

$$y_1 = \frac{H_1}{4EI{\beta_1}^3} \tag{33}$$

$$H_2 = \frac{2\beta_1 Z_n \sigma_n}{\sqrt{1 + (\beta_1 h)^2 exp[-tan^{-1}(1/\beta_1 h)]}} \tag{34}$$

$$y_2 = \frac{(1 + \beta_1 h)^3 + 2}{12EI{\beta_1}^3} H_2 \tag{35}$$

$$H_3 = \sqrt{\frac{6/\alpha^2 - \sqrt{36/\alpha^4 - 24N/\alpha^3}}{2}} \tag{36}$$

$$y_3 = \frac{(1 + \beta_1 h)^3 + 1/2}{3EI{\beta_1}^3} H_3 \tag{37}$$

Where, $\alpha = \frac{(1+\beta h)^2}{2EI\beta^2}$.

2.3.2.2. Decayed wood and no damage nail

Fig.10 is a schematic of decayed wood and no damage nail using steel plate as the side material. In this case, first, the nail head yields in the state where the nail head is non-protruding and fixed. Then the nail body yields in the no damage part of wood or at the boundary between the no damage part and the decay part of wood in the state where the nail head is non-protruding and free, and finally the nail pulls out. The nail head conditions for pulling out are protruding and free when the yield of nail body occurs in the no damage part of wood, and non-protruding and free when it occurs at the boundary between the no damage part and the decay part of wood. The horizontal load and horizontal displacement of the nail head at these times are expressed by equation (38) ~ (50), respectively.

https://doi.org/10.52202/069179-0344

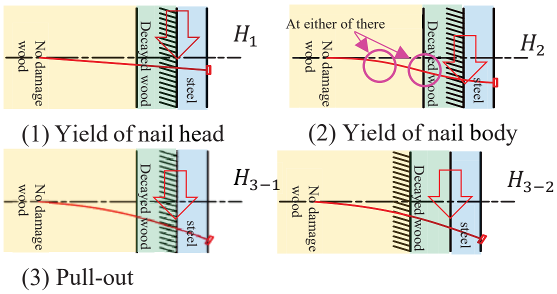

Figure 10: *Decayed wood and no damage nail*

$$H_1 = -\frac{2\beta_1 b_3 h_1}{b_1 h_1 - 8h_2} Z_n \sigma_n \quad (38)$$

$$y_1 = \frac{b_2 h_1 + 8h_3}{4EI\beta_1^{\ 3} b_3 h_1} H_1 \quad (39)$$

$$H_{2-1} = \frac{\beta_1 Z_n \sigma_n (f_5 sin(\beta_2 \ell) + f_6 cos(\beta_2 \ell)) h_4}{2\beta_2^{\ 2}(f_3^{\ 2} + f_4^{\ 2}) sin(\beta_2 \ell_m)} e^{\beta_2 \ell_m - \beta_2 \ell} \quad (40)$$

$$\ell_{m-1} = \frac{1}{\beta_2} tan^{-1}\left(-\frac{f_5 sin(\beta_2 \ell) + f_6 cos(\beta_2 \ell)}{f_6 sin(\beta_2 \ell) - f_5 cos(\beta_2 \ell)}\right) \quad (41)$$

$$y_{2-1} = \frac{b_4 h_4 + 4h_5 - 4h_6}{2EI\beta_1^{\ 3} b_2 h_4} H_{2-1} \quad (42)$$

$$H_{2-2} = \frac{\beta_1 Z_n \sigma_n h_4}{2\beta_2^{\ 2} f_4} \quad (43)$$

$$y_{2-2} = \frac{b_4 h_4 + 4h_5 - 4h_6}{2EI\beta_1^{\ 3} b_2 h_4} H_{2-2} \quad (44)$$

$$H_{3-1}{}' = \sqrt{\frac{6/\alpha'^2 - \sqrt{36/\alpha'^4 - 24P_d{}'/\alpha'^3}}{2}} \quad (45)$$

$$y_{3-1}{}' = \frac{1}{2EI\beta_2^{\ 3}} H_{3-1}{}' \quad (46)$$

$$H_{3-1} = \frac{P_d + H_{3-1}{}' sin(\gamma_2 H_{3-1}{}')}{sin(\gamma_1 H_{3-1}{}') - H_{3-1}{}' \alpha_2 cos(\gamma_2 H_{3-1}{}')} \quad (47)$$

$$y_{3-1} = \frac{\beta_1^{\ 2} b_4 + R_1 + R_3}{2EI\beta_1^{\ 5} b_2} H_{3-1} + \frac{R_2 + R_4}{2EI\beta_1^{\ 2}\beta_2^{\ 3} b_2} H_{3-1}{}' + y_{3-1}{}' \quad (48)$$

$$H_{3-2} = \sqrt{\frac{6/\alpha^2 - \sqrt{36/\alpha^4 - 24N/\alpha^3}}{2}} \quad (49)$$

$$y_{3-2} = \frac{(1+\beta_1 \hbar)^3 + 1/2}{3EI\beta_1^{\ 3}} H_{3-2} \quad (50)$$

Where, $\alpha' = \frac{1}{2EI\beta^2}$, $\alpha_1 = \frac{\beta_1^{\ 2} b_1 + 2R_5 - 2R_7}{2EI\beta_1^{\ 4} b_2}$, $\alpha_2 = \frac{S_1 - S_3}{2EI\beta_1^{\ 3}} \times \frac{\beta_2 sin(\beta_2 \ell_m)}{f_5 sin(\beta_2 \ell) + f_6 cos(\beta_2 \ell)}$, $\gamma_1 = \frac{R_6 + R_8}{2EI\beta_1 \beta_2^{\ 3} b_2}$, $\gamma_2 = \frac{S_2 + S_4}{2EI\beta_2^{\ 2}} \times \frac{sin(\beta_2 \ell_m)}{f_5 sin(\beta_2 \ell) + f_6 cos(\beta_2 \ell)}$, $\alpha = \frac{(1+\beta\hbar)^2}{2EI\beta_1^{\ 2}}$

2.3.2.3. Decayed wood and rusted nail

Table 10 shows the nail head conditions and joint behavior at the situation of no damage wood and rusted nail and decayed wood and no damage nail. And Fig. 11 shows experimental results and estimates at the situation. From Fig.11, the formulas are correct because the experimental result and the estimated value match. Therefore, considering these results, nail head conditions and nail joint behavior are expected when wood decay and nail rust occur in combination. The first change point of the load-deformation relationship is the point where the plywood yields when the nail head condition is non-protruding and fixed. This is because, in wooden houses, plywood is used as the side material, so the nail head will not yield. Next, the second change point is the point where the nail yields in the no damage part of the wood or at the boundary between the no damage part and the decayed part of the wood when the nail head condition is protruding and fixed. The reason why the nail head condition is protruding is that the deflection angle of the nail head increase due to the yield of the plywood, and it is thought that it protrudes. Finally, the third change point is the point at which the nail pulls out, breaks, or punching out when the nail head condition is protruding and free. The horizontal load and horizontal displacement of the nail head at these times are expressed by equation (51) ~ (58), respectively. There are summarized as shown in Fig.12. Fig. 13 shows the behavior of the nail joint for each degree of deterioration calculated using these results.

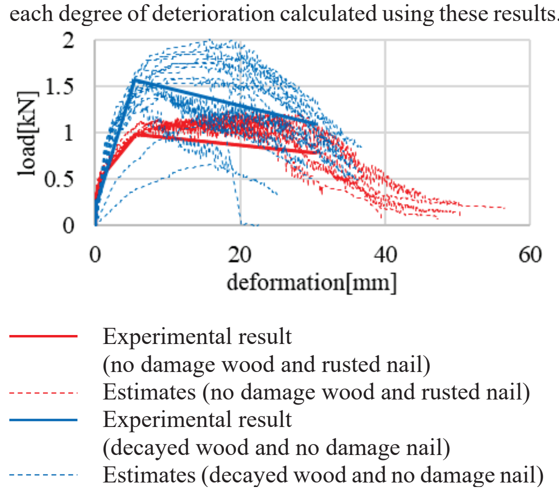

Figure 11: *Experimental results and estimates with rusted nail or wood decayed*

$$H_1 = \frac{\sigma_{yp} \times A_p}{2} \quad (51)$$

$$y_1 = \frac{b_2 h_1 + 8h_3}{4EI\beta_1^{\ 3} h_1 b_3} H_1 \quad (52)$$

Table 10: Expected nail head conditions and nail joint behaviour with rusted nail or decayed wood

	No damage wood and rusted nail		Decayed wood and no damage wood			
	Nail head condition	Behavior	Nail head condition		Behavior	
1	Non-protruding/ fixed	Yield of plywood	Nail pulls out		Yield of nail head	
2	Protruding/ fixed	Yield of nail body	Non-protruding/ free		Yield of nail body	
					At the no damage part	At the boundary between the no damage part and the decay part
3	Protruding/ free	Nail pulls out, breaks, or punching out	Non-protruding/ free with pin support	Protruding/ free	Nail pulls out	

$$H_{2-1} = \frac{4\beta_1 Z_n \sigma_n t_1(\beta_1 \hbar T_1 + T_2) W_1 e^{\beta_2(\ell_m - \ell)}}{Y_1 sin(\beta_2 \ell_m)} \quad (53)$$

$$H_{2-2} = -\frac{4\beta_1 Z_n \sigma_n t_1(\beta_1 \hbar T_1 + T_2)}{{\beta_1}^2 \hbar^2 U_2 + \beta_1 \hbar U_4 + U_6} \quad (54)$$

$$y_2 = \frac{H_2}{12EI{\beta_1}^3 t_1(\beta_1 \hbar T_1 + T_2)} \times \left\{ \begin{array}{c} {\beta_1}^4 \hbar^4 t_1 T_1 + 4{\beta_1}^3 \hbar^3 t_1 T_2 \\ +3{\beta_1}^2 \hbar^2 (t_1 T_3 + t_2 T_2 + t_3 T_1) \\ +3\beta_1 \hbar (t_2 T_3 + t_4 T_1) + 3(-t_3 T_3 + t_4 T_2) \end{array} \right\} \quad (55)$$

$$H_3 = \sqrt{\frac{6/\alpha^2 - \sqrt{36/\alpha^4 - 24N/\alpha^3}}{2}} \quad (56)$$

$$y_{3-1} = \frac{H_3}{12EI{\beta_1}^3 t_1 T_1}\{4{\beta_1}^3 \hbar^3 t_1 T_1 + 12{\beta_1}^2 \hbar^2 t_1 T_2 + 6\beta_1 \hbar (t_1 T_3 + t_2 T_2 + t_3 T_1) + 3(t_2 T_3 + t_4 T_1)\} \quad (57)$$

$$y_{3-2} = \frac{H_3}{3EI{\beta_2}^3}\{(1 + \beta_2 \hbar)^3 + 1/2\} \quad (58)$$

Where, $\alpha_1 = \frac{{\beta_1}^2 \hbar^2 T_1 + 2\beta_1 \hbar T_2 + T_3}{2EI{\beta_1}^2 T_1}$, $\alpha_2 = \frac{(\beta_2 \hbar + 1)^2}{2EI{\beta_2}^2}$.

3 MODELING AND ANALYSIS

3.1 OUTLINE

Based on the estimated value by the formula in 2.3.2, the elastoplastic analysis of the plywood bearing wall model is carried out using the analysis software SNAP. The model is shown in Fig.14. To analyze the strength of the plywood bearing wall based on the estimated shear resistance of the nail joint, two frame models are connected with a spring 1, and the estimated value calculated in 2.3.2 is input to spring 1. Further, one of the frame models a wooden frame in the plywood bearing wall and the other models a frame when the structural plywood is expanded using brace expansion.

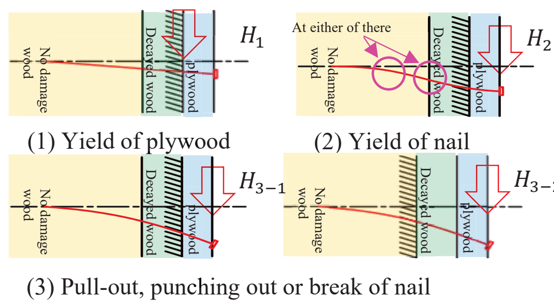

Figure 12: Decayed wood and rusted nail

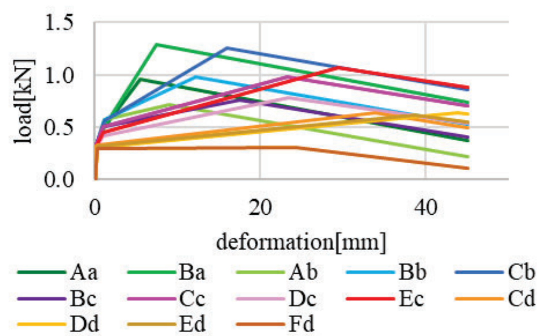

Figure 13: The performance of nails in each deterioration degree

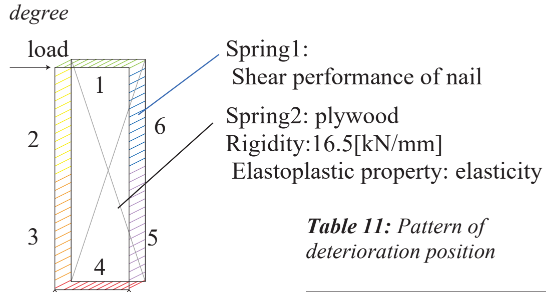

Figure 14: Model of wall and location of deterioration

Table 11: Pattern of deterioration position

Pattern	Deterioration position
(α)	No damage
(β)	4
(γ)	5,6
(ω)	1,2,6

https://doi.org/10.52202/069179-0344

3.2 LOCATION OF DETERIORATION

The plywood bearing wall is divided into areas as shown in Fig14, and the deterioration position that is likely to occur is divided into patterns assuming deterioration in the house. This is shown in Table 11. The analysis is carried out when the nail joint at these 4 pattern positions become about 13 levels of deterioration shown in the shaded portion of Table 2.

3.3 ANALYSIS RESULT

Fig.15(α) shows the analysis result and the experimental result of the past[7] with the no damaged nail and wood. The analysis result agrees well with the experimental result. Next, the analysis results of patterns (β), (γ) and (ω) are also shown in Fig.15. In the case of (β), the load-deformation relationship is almost the same regardless of the degree of deterioration of the foundation. In the case of (γ), the deformation increases as the deterioration progresses, but there is no significant effect on the maximum strength. In the case of (ω), the maximum strength and rigidity after yield decreases remarkably as the deterioration progresses.

4 CONCLUSIONS

The structural performance of plywood bearing wall with the nails rusted and columns decayed can be predicted by deterioration degree of nails and columns. The maximum strength doesn't decrease remarkably when only the foundation of plywood bearing wall deteriorates. On the other hand, when the pillar deteriorates, the rigidity after yield is greatly reduced. In addition, even if the wood decay a little, the strength increases due to the influence of rusting of the nail, and it decreases when further deterioration progresses.

ACKNOWLEDGEMENT

This study was carried out with support from the Asahi Glass Foundation.

REFERENCES

[1] Hiroto Imamura, Makoto Kiguchi, Akio Okuro: The Deteriorating Circumstances of Wood Viewed from the Deterioration of Nails in the Exterior Wall of Wooden Houses, Bull. For. & For. Prod. Res. Inst, No.345, pp.101-149, 1987

[2] Hiroki Ishiyama, Mikio Koshihara: Experimental study on the performance of the nailed joint with rust -Study on the structural performance of wooden houses when deteriorated(Part 1)-, Journal of Structural and Construction Engineering, Vol.74, No.646, pp.2281-2289, 2009.12.

[3] Nakaba Wada, Hiroki Ishiyama: The Structural Performance of the Nail Driven into the Decayed Wood. Summaries of technical papers of annual meeting, Architectural Institute of Japan (Hokuriku), September 2019.

[4] Kotaro Kawano, Takumi Nakahata, Yuhei Mouri, Takuro Mori, Yoshiyuki Yanase, Kei Tanaka, Masafumi Inoue: The study on the evaluation of the remaining seismic performance of wooden buildings subjected to biodegradation, AIJ Kyushu chapter architectural research meeting, 2016.3

[5] Qingjun Meng, Takuro Hirai, Akio Koizumi: Frictional coefficients between timber and some structural sheet materials, Journal of the Japan Wood Research Society, Vol.54, No.5, pp.281-288, 2008

[6] Architectural Institute of Japan: Recommendations for design of building foundation(2003 Edition), pp.262-297

[7] Hiroki Ishiyama, Mikio Koshihara: Experimental study on the performance of the shear wall with the nails rusting, Journal of Structural and Construction Engineering, Vol.77, No.676, pp.911-918,

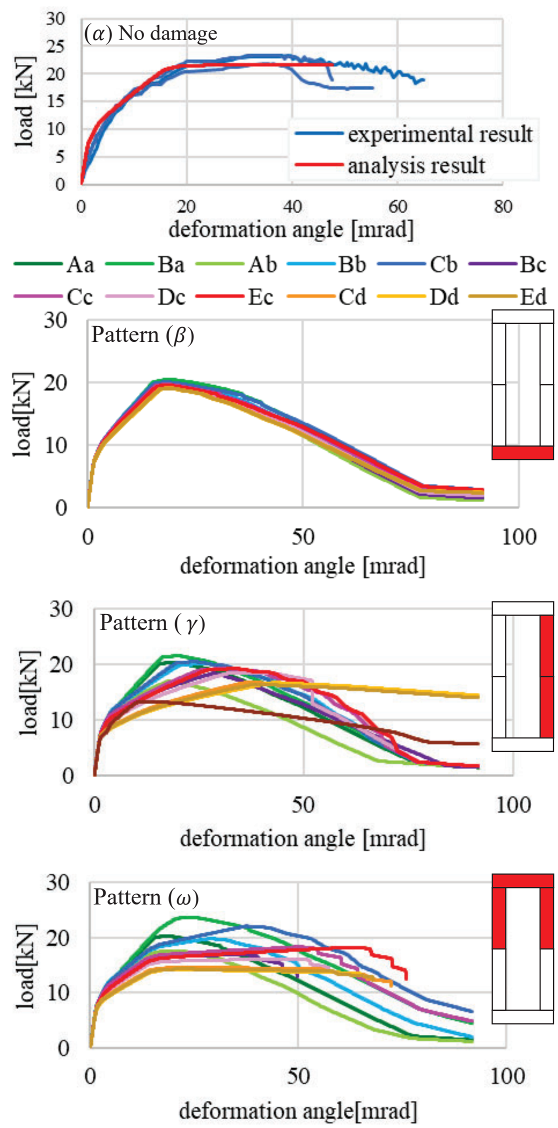

Figure 15: *The analysis result and the experimental result*